

phys. stat. sol. (b) **220**, 141 (2000)

Subject classification: 63.22.+m; 78.30.Fs; S7.11; S7.15

Micro-Raman Studies of $\text{Al}_x\text{Ga}_{1-x}\text{P}/\text{GaP}$ Graded Structures

E. ZAMORA (a), P. DÍAZ (a), S. JIMÉNEZ-SANDOVAL (b), C. GONZÁLEZ-RAÑA (a),
T. A. PRUTSKIJ (c), V. MISHURNII (d), and A. MERKULOV (e)

(a) *Laboratory of Semiconductors, IMRE, Faculty of Physics, University of Havana, Cuba*

(b) *Laboratory of Materials Research, CINVESTAV, Autonomous University of Querétaro, Mexico*

(c) *Center of Research in Semiconductor Devices, ICUAP, BUAP, Puebla, Pue., Mexico*

(d) *Institute of Optical Communication, Autonomous University of San Luis de Potosí, Mexico*

(e) *SEES, Department of Electrical Engineering, CINVESTAV-IPN, Mexico D.F., Mexico*

(Received November 1, 1999)

We report applications of the micro-Raman technique to study the compositional dependence of phonon modes in graded $\text{Al}_x\text{Ga}_{1-x}\text{P}$ layers. The dependence of the phonon frequencies on the Al content was monitored in a single sample for two different crystallographic orientations. The measured compositional dependence of the LO and TO phonon frequencies are in good agreement with results of calculations based on the Modified Random Element Isodisplacement (MREI) model. The Raman spectra of the samples reveal also the existence of other features due to disorder.

In this paper, we discuss applications of the micro-Raman technique (MR) to graded semiconductor alloy samples. This technique allows one to obtain information on surfaces at two different crystallographic orientations, namely, the [100] sample surface and the cleaved facet [110], and the graded composition of the sample. Thus, the micro-Raman method allowed us to gain a rapid qualitative evaluation of the composition profile, as well as, to probe the quality of the layer/substrate interface. Previous reports on MR spectroscopy in semiconductors [1, 2] have not considered these aspects in detail.

First-order Raman scattering from lattice vibrations of $\text{Al}_x\text{Ga}_{1-x}\text{P}$ alloys has been reported in [3 to 5]. These studies were performed for (100)-oriented layers in the backscattering geometry using conventional Raman scattering.

The $\text{Al}_x\text{Ga}_{1-x}\text{P}$ layers were grown by liquid phase epitaxy on n-type GaP ($N_d = 4.0 \times 10^{17} \text{ cm}^{-3}$) substrates oriented in the [100] direction with a small (4° to 8°) misorientation towards the (110) plane. The layers exhibit a varying Al concentration ($0 \leq x \leq 0.7$) and thickness ($3 \mu\text{m} \leq d \leq 12 \mu\text{m}$). The Al composition profile was determined by SIMS (Secondary Ion Mass Spectroscopy). The MR experiments were carried out at room temperature using a LabRAM Dilor micro-Raman system. The samples were excited with 20 mW of the 632.8 nm line of a He-Ne laser and the scattered light was detected using a monochromator and a low noise CCD. The measurements were performed in the backscattering geometry. The various experimental configurations are described in Fig. 1.

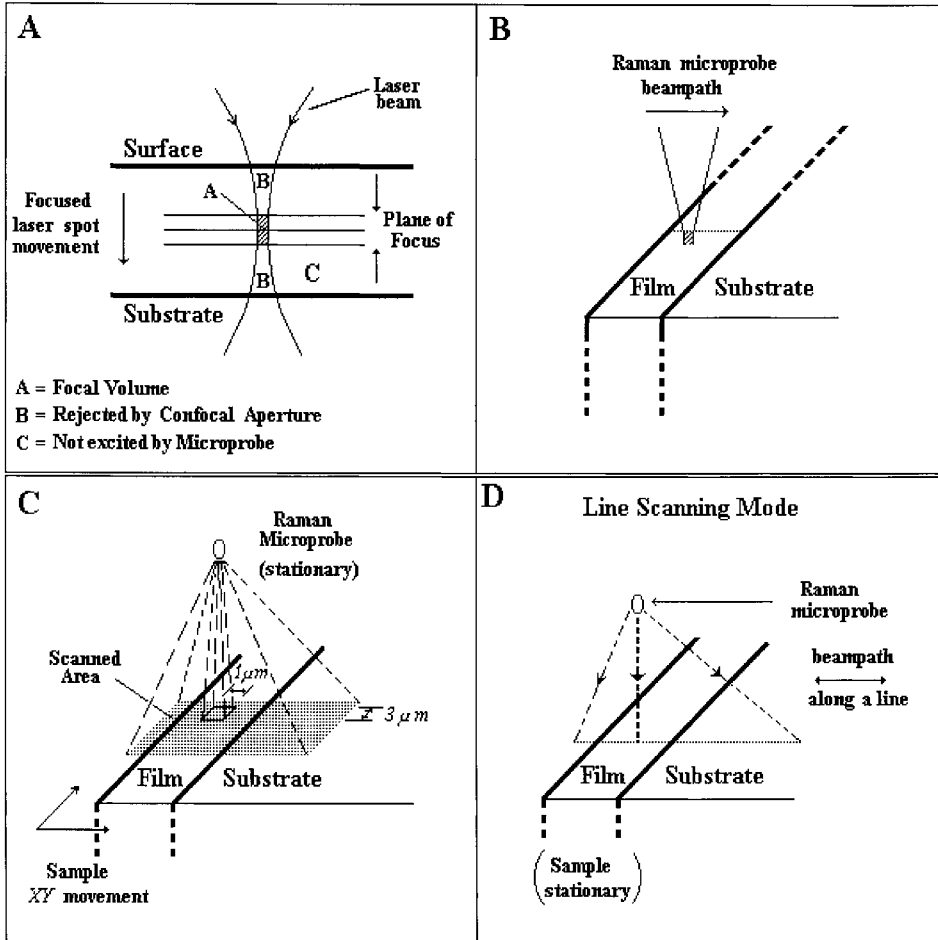


Fig. 1. Experimental configurations. A: confocal mode, the sample is illuminated on the (100) surface stepping $1 \mu\text{m}$ in depth; B: the sample is illuminated on the (110) cleaved facet in $1 \mu\text{m}$ steps; C: spectral image mode on the cleaved facet; D: line scanning mode along the (110) cleaved facet

In Fig. 1A, the Al composition was studied by scattering off the [100] surface of the sample toward the epilayer/substrate interface with the laser beam focused with the aid of a confocal microscope in $1 \mu\text{m}$ steps. In this mode, the system allows one to achieve an in-depth spatial resolution of $\approx 3 \mu\text{m}$ centered on the focal plane while the lateral spatial resolution is of $\approx 1 \mu\text{m}$. In Fig. 1B, the laser beam is focused near the layer/substrate interface and tracks down along the cleaved facet toward the surface of the sample in $1 \mu\text{m}$ steps. This experiment was carried out at the best spatial resolution achievable with the instrument, $\approx 1 \mu\text{m}$. In Fig. 1C, the AlGaP/GaP interface was analyzed by scanning an area of $20 \times 45 \mu\text{m}^2$. This was achieved by displacing the sample with a computer-controlled XY stage. The total area was divided into $3 \mu\text{m}^2$ cells and for each cell a Raman spectrum was obtained. Finally, in Fig. 1D, we used the line scanning mode, in which the laser beam is scanned across the film/substrate interface

while the sample remains stationary. Here it was possible to obtain an average Raman spectrum for each $1 \mu\text{m}$ segment.

In experiments C and D the signal associated with the $\text{TO}(\Gamma)$ AIP-like phonons was monitored to get information about the Al compositional profile of the film during growth, as shown in Fig. 2. This approach has the advantage that it does not require a vacuum environment, it is non-destructive and less expensive than other techniques traditionally employed to probe chemical compositions.

The micro-Raman spectra of our samples are characterized by: (i) a two-mode behavior of the optical phonon and its dependence on the Al content, (ii) the appearance of forbidden peaks possibly due to substrate misorientation, structural disorder and/or fluctuations of the periodic potential leading to a break down of the Raman selection rules, (iii) the Raman contribution from the substrate which is due to the transparency

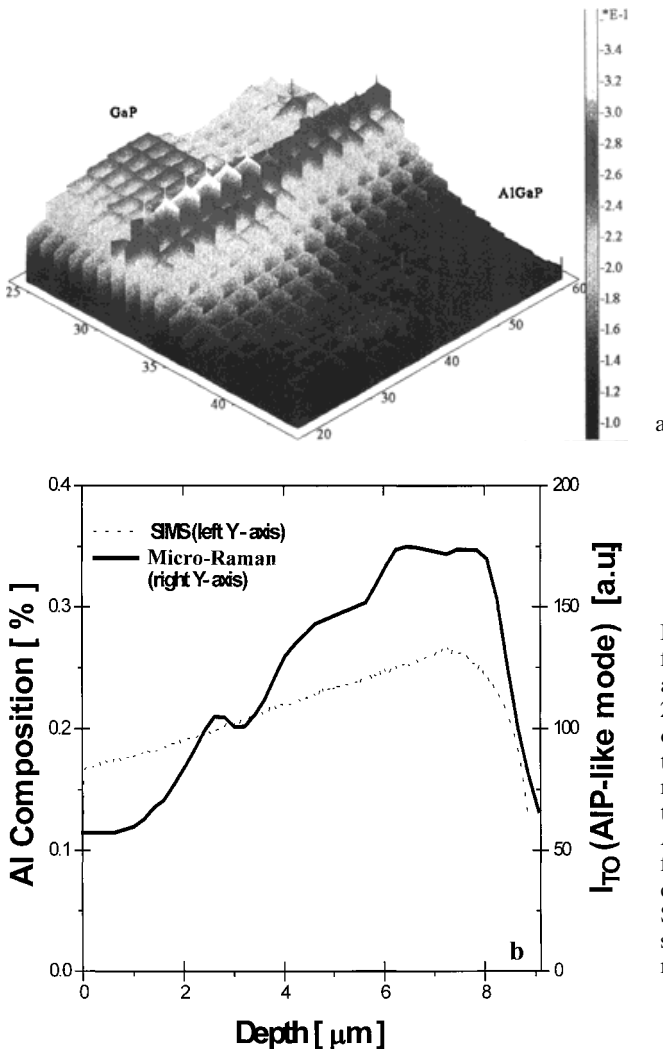


Fig. 2. a) Compositional profile from experiment C. Spectral image obtained from an area of $20 \times 45 \mu\text{m}^2$ taken from the edge of the sample. The data shows intensity of the $\text{TO}(\Gamma)$ Al-like phonon normalized to the intensity of the $\text{TO}(\Gamma)$ GaP-like phonon. b) Aluminum compositional profile from experiment D (solid line), in comparison with that obtained by SIMS (dashed line). The Raman system was used in line scanning mode (experiment D)

of GaP to the 6328 Å laser line, and (iv) the appearance of second order Raman peaks also from the substrate.

The Raman spectra from sample in experiment A are shown in Fig. 3a. The dominant features are the allowed GaP-like (392 to 396 cm^{-1}) and AIP-like (456 to 463 cm^{-1}) phonon modes of the film. As expected, one can clearly see the decrease of the GaP-like LO(Γ) phonon frequency as the Al composition increases, while the opposite behavior is observed for the frequency of the AIP-like mode. The peak at 366 cm^{-1} is due to the TO(Γ) phonon of the substrate, its intensity increases as the Raman probe gets closer to the substrate. Although this peak is normally forbidden in this configura-

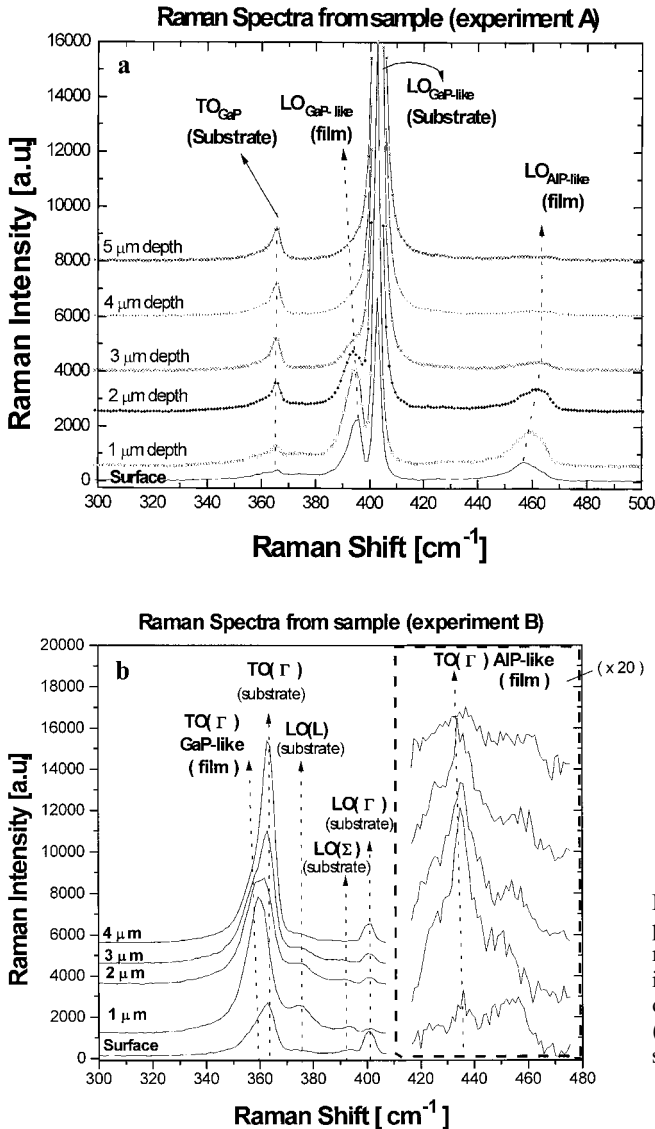


Fig. 3. a) Raman spectra of sample in the confocal mode (experiment A). Data are shown for various laser focal plane penetration depths. b) Raman spectra off the (110) plane of the cleaved facet in sample (experiment B)

tion, it appears because the backscattering geometry is not exactly met. Additionally, not shown in the figure, we find less intense peaks at 212 (DALA(X, K)), 250 (DALA(X)), 715 ($2 \times \text{TO(L)}$), 750 ($\text{LO}(\Sigma) + \text{TO(L)}$) and 780 cm^{-1} ($2 \times \text{LO}(\Sigma)$) due to second-order Raman scattering from the substrate.

All the features observed in type A experiments were also seen in experiments of type B, shown in Fig. 3b. However, experiments of type B give richer spectra with additional features. In particular, some of the spectra reveal a low intensity peak at $\approx 377 \text{ cm}^{-1}$, that is attributed to LO(L) phonons of the substrate. Associated with this frequency, there is a strong peak in the phonon density of states at the L point of the Brillouin zone [6]. We note that this peak appears in experiment of type A in other samples. In Fig. 3b, we also observe the $\text{LO}(\Sigma)$ mode [7] at 390 cm^{-1} and the $\text{TO}(\Gamma)$ AIP-like of the $\text{Al}_x\text{Ga}_{1-x}\text{P}$ film at about 440 cm^{-1} . In experiment B, the selection rules are such that the intensity of the $\text{TO}(\Gamma)$ peaks is much greater than that of the $\text{LO}(\Gamma)$ phonon.

To improve the accuracy of our analysis, the spectra taken at different locations in the sample for experiments A and B were fitted with multi-Lorentzian lines. The fitted frequencies were correlated with the Al composition profile obtained from SIMS experiments. Using both sets of results, we obtain the compositional dependence of the $\text{Al}_x\text{Ga}_{1-x}\text{P}$ optical modes depicted in Fig. 4. For comparison, the calculated dependences appear also in the figure. We have chosen the widely used MREI model to describe the two-phonon mode behavior of III-V mixed crystals with reasonable accuracy [8]. As expected, this model describes well the experimental results. In Fig. 4 we also compare our results with those reported in Ref. [9]. As can be observed, the results of the two calculations are very similar. The small differences arise likely from the fact that Ref. [9] uses a six-parameter MREI model while we used only four parameters with different input values.

In conclusion, we have shown that MR in graded samples can be used to study the lattice dynamics of semiconductor alloys. Our approach allows us to monitor different crystallographic orientations and compositional profiling without special preparation.

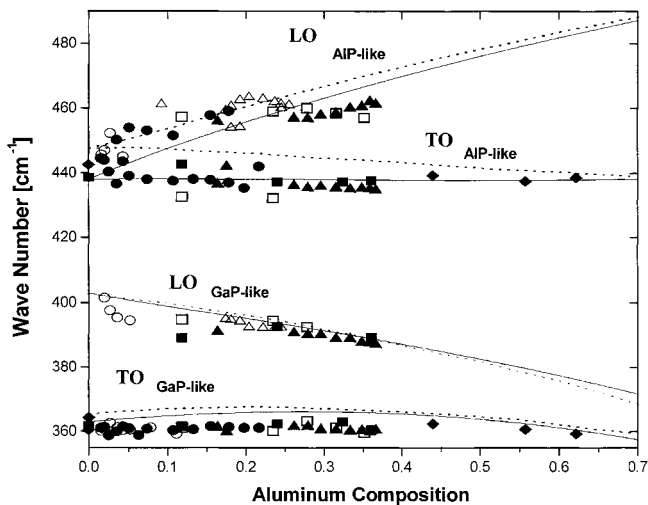


Fig. 4. Compositional dependence of Raman frequencies calculated using a four-parameter MREI model (solid lines), those reported in Ref. [9] (dotted lines) and our experimental data. The different symbols correspond to different samples in experiments A (open symbols) and B (solid symbols)

References

- [1] F. A. PONCE, J. W. STEEDS, C. D. DYER, and G. D. PITT, *Appl. Phys. Lett.* **69**, 2650 (1996).
- [2] J. GERSTNER, J. M. SCHNEIDER, C. EHRET, W. LIMMER, R. SAUER, and H. HEINECKE, *Appl. Phys. Lett.* **70**, 69 (1997).
- [3] D. P. BOUR, J. R. SHEALY, A. KASENZOV, and F. POLLAK, *J. Appl. Phys.* **64**, 6456 (1988).
- [4] B. KH. BAIRAMOV, V. N. BESSOLOV, E. JAHNE, YU. P. YAKOLEV, V. V. TODOROV, and Sh. B. UBALDULLAEV, *Soviet Tech. Phys. Lett.* **6**, 618 (1980).
- [5] G. ARMELLES, J. M. CALLEJA, and E. MUÑOZ, *Solid State Commun.* **65**, 779 (1988).
- [6] N. D. STRAHM and A. L. MCWHORTER, *Proc. Internat. Conf. LSSS*, Ed. G. B. Wright, Springer, New York 1968 (p. 455).
- [7] B. H. BAIRAMOV, V. K. NEGODUYKO, and Z. M. HASHKOZEV, *Proc. 12th Internat. Conf. Physics of Semiconductors*, Ed. M. H. PILKUHN. Teubner, Stuttgart 1974 (p. 445).
- [8] Y. T. CHERNG, D. H. JAW, M. J. JO, and G. B. STRINGFELLOW, *J. Appl. Phys.* **65**, 3285 (1988).
- [9] D. N. TALWAR and T. D. FANG, *Phys. Rev. B* **41**, 3746 (1990).